Supporting Information for

A Mono-Copper Doped Undeca-Gold Cluster with Up-converted and Anti-Stokes Emissions of Fluorescence and Phosphorescence

Haiming Wu,[#a] Ye-Guang Fang,[#b] Rajini Anumula,[#a] Gaya N. Andrew,[a] Ganglong Cui,*[b] Weihai Fang,[b] Zhixun Luo,*[a] and Jiannian Yao[a]

[a] *Beijing National Laboratory for Molecular Sciences (BNLMS) and State Key Laboratory for Structural Chemistry of Unstable and Stable Species, Institute of Chemistry, Chinese Academy of Sciences, Beijing 100090, China.*

[b] *Key Laboratory of Theoretical and Computational Photochemistry, College of Chemistry, Beijing Normal University, Beijing 100875, China.*

** Correspondence. Email: zxluo@iccas.ac.cn (Z.L.); ganglong.cui@bnu.edu.cn (G.C.)*

[#] *These authors contributed equally to this paper and share first authorship.*

Contents

S1. Experimental and theoretical methods

Chemicals. All the reagents used in this study are of analytical grade and used without further purification. Copper (II) acetate [$Cu(OAc)_2$, 99% purity] and cupric nitrate [$Cu(NO_3)_2$, 99% purity] were purchased from Alfa Aesar Chemical Reagent; hydrogen tetrachloroaurate ($HAuCl_4 \cdot 4H_2O$, 99.9% purity), 2-pyridinethiol (C_5NH_5S, 99% purity) and triphenylphosphine ($C_{18}H_{15}P$, 95% purity, 'PPh_3' for short below) are from J&K Scientific Chemical Company; sodium borohydride ($NaBH_4$, 98% purity) and triethylamine ($C_6H_{15}N$, A.R.) from Acros Organics Chemicals. The solvents dichloromethane (DCM for short below), methanol, ethanol, n-pentane, diethyl ether and n-hexane were purchased from Beijing Chemical Reagent Co. Ltd. The distilled water used throughout all experiments was purified by a Millipore system.

Synthesis of precursor $AuClPPh_3$. In this study, typically the starting material, $HAuCl_4 \cdot 4H_2O$ (1 g), was dissolved in absolute ethanol (80 mL) which was taken in a round-bottom flask. Then PPh_3 (1.33 g) was dissolved in 40 mL ethanol which was then added to the above gold mixture under constant stirring for about 30 mins at room temperature, until the precipitates formed. Subsequently, the resulting solution was filtered and washed with diethyl ether three times, and finally dissolved in DCM. White crystals of $AuClPPh_3$ were obtained after layering the filtrate with excess pentane. As the $AuClPPh_3$ is a light sensitive chemical, all the above operations were carried out in dark conditions.

Synthesis of $Au_{11}Cu_1$ nanocluster. In a glass vial, $Cu(OAc)_2$ (30 mg) and $Cu(NO_3)_2$ (30 mg) were dissolved in methanol under sonication. To this solution, 50 mg of as-prepared $AuClPPh_3$ precursor which dissolved in DCM was added under an ice-bath. A freshly prepared solution SPy (~ 50 mg) and PPh_3 (~ 31 mg) in DCM was added, respectively. After stirring (~ 20 mins), ~ 4 mL of $NaBH_4$ and ~ 0.4 mL of triethylamine were added together quickly to the above solution. This solution was kept under stirring and aged for one day at 0 ^oC and then was washed several times with distilled water for one- or two-days using centrifuge. Afterwards, the solution was centrifuged by rotavapor and the obtained brown extract was thus crystalized in DCM/hexane (1:4) at 4 ^oC and kept for black single crystal growth for 13 days. The yield of $Au_{11}Cu_1$ was up to ~40 % and the washed nanocluster is stored at 4 ^oC found to be highly stable for several months.

Characterization. The single-crystal X-ray diffraction (XRD) data of the synthesized bimetallic $Au_{11}Cu_1$ nanocluster was measured on an XtaLAB AFC10 (RCD3) fixed-chi single crystal X-ray diffractometer with Mo Kα radiation (λ=0.71073 Å) at 103.15 K. Single crystal structure was solved by direct methods and refined with full-matrix-least-squares on F^2. Electrospray ionization time-of-flight mass spectrometry (ESI-TOF-MS) measurements were conducted by a MicroTOF-QIII High-resolution Mass Spectrometer in the negative ionization mode. The UV-Vis absorption spectra were collected using an UV-3600 Shimadzu UV-Vis-NIR Spectrophotometer. Photoluminescence spectra were recorded by a Horiba Scientific Fluoromax-4 spectrofluorometer.

S2. Experimental details

- **Single crystal parsing**

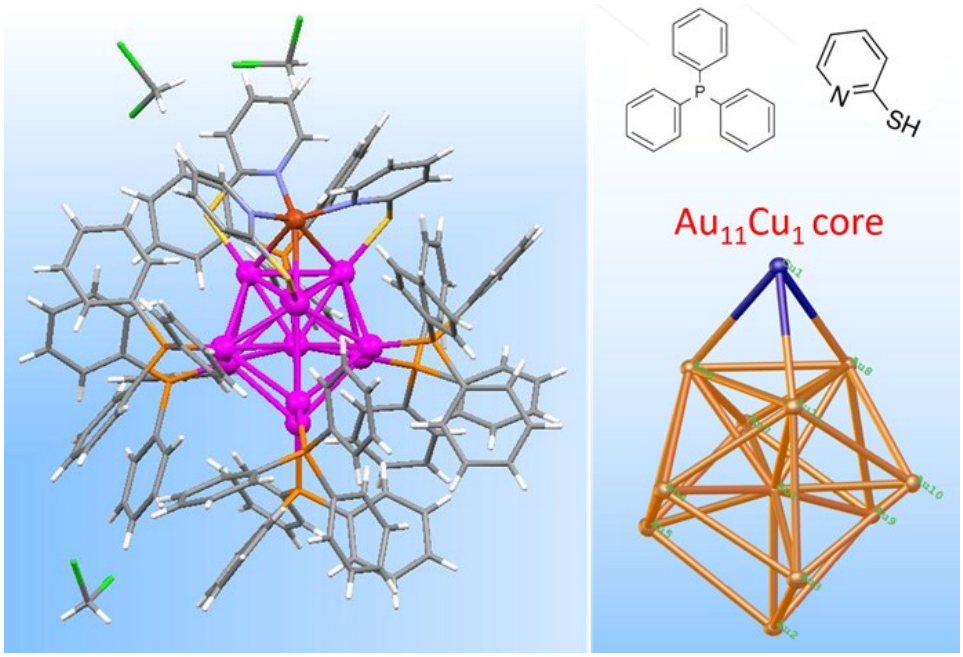

Fig. S1 Single crystal parsing of the synthesized $[Au_{11}Cu_1(PPh_3)_7(SPy)_3]^+$ cluster, where the three Au-Cu edges are protected by 3-SPy ligands via one leg of N atoms bonding to Cu and the other leg of sulfur bonding to Au (No. 6, 8, 11); while the other sever surface Au atoms (except the central Au1) are protected by 7 PPh_3 ligands.

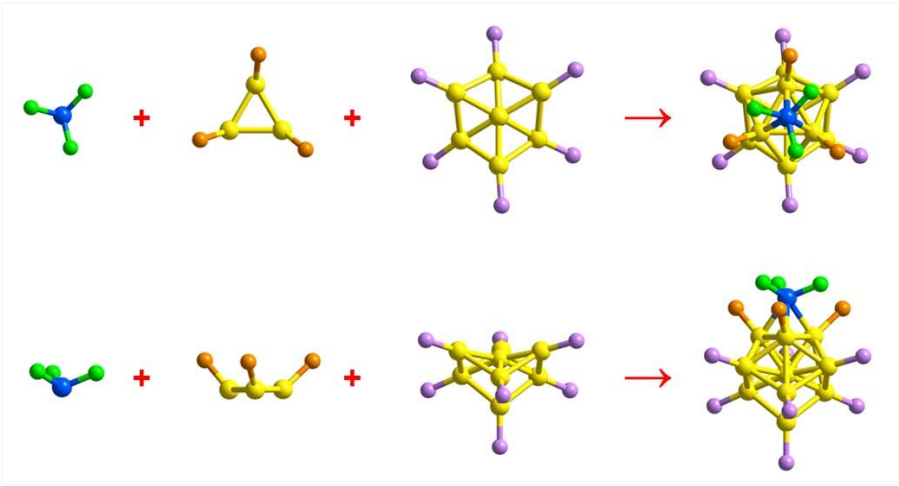

Fig. S2 The $Au_{11}Cu_1N_3S_3P_7$ unit of the nanocluster. Au, yellow; Cu, blue; S, orange; P, violet; N, green; Cl, light blue. For clarity, C and H are omitted.

Table S1 Crystallographic data for compound $Au_{11}Cu_1$ nanocluster.

Empirical formula	$C_{144}H_{123}Au_{11}Cl_6CuN_3P_7S_3$	
Formula weight	4651.29	
Temperature	103.15 K	
Wavelength	0.71073 Å	
Crystal system	Monoclinic	
Space group	P 1 21/c 1	
Unit cell dimensions	a = 17.0278(2) Å	α = 90°
	b = 37.9099(4) Å	β = 99.3170(10)°
	c = 26.2407(3) Å	γ = 90°
Volume	16715.5(3) $Å^3$	
Z	4	
Density (calculated)	1.848 Mg/m^3	
Absorption coefficient	9.979 mm^{-1}	
F(000)	8644	
Crystal size	0.759 x 0.259 x 0.225 mm^3	
Theta range for data collection	1.620 to 27.485°.	
Index ranges	-22<=h<=22, -49<=k<=49, -33<=l<=34	
Reflections collected	225567	
Independent reflections	38285 [R(int) = 0.0869]	
Completeness to theta = 25.242°	100.0 %	
Absorption correction	Semi-empirical from equivalents	
Max. and min. transmission	1.00000 and 0.01073	
Refinement method	Full-matrix least-squares on F^2	
Data / restraints / parameters	38285 / 36 / 1575	
Goodness-of-fit on F^2	1.049	
Final R indices [I>2sigma(I)]	R1 = 0.0442, wR2 = 0.1106	
R indices (all data)	R1 = 0.0513, wR2 = 0.1140	
Extinction coefficient	n/a	
Largest diff. peak and hole	2.406 and -2.994 e.$Å^{-3}$	

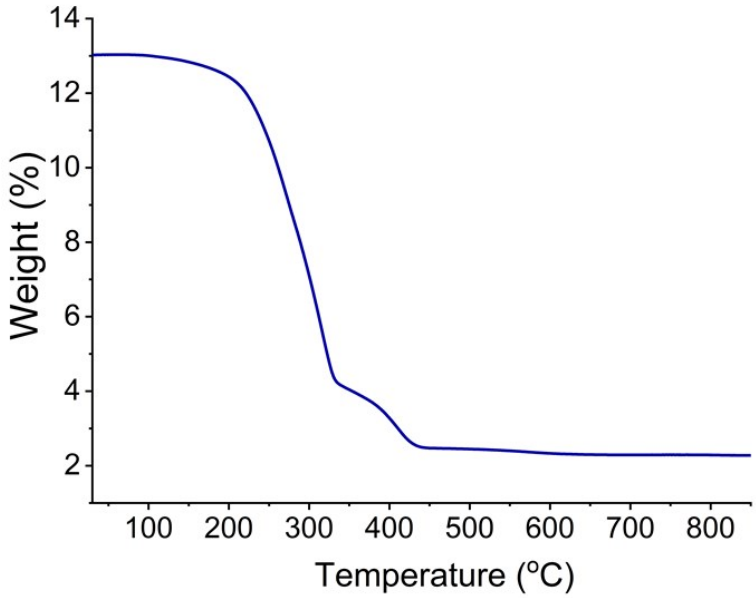

Fig. S3 The TG-DTA curve of $[Au_{11}Cu_1(PPh_3)_7(SPy)_3]^+$ cluster.

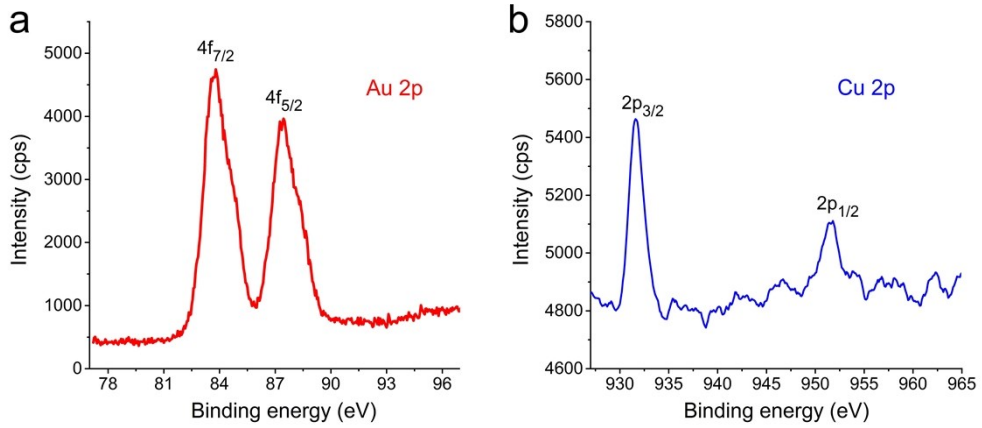

Fig. S4 XPS patterns of Au 4f (a) and Cu 2p (b) of $[Au_{11}Cu_1(PPh_3)_7(SPy)_3]^+$ cluster.

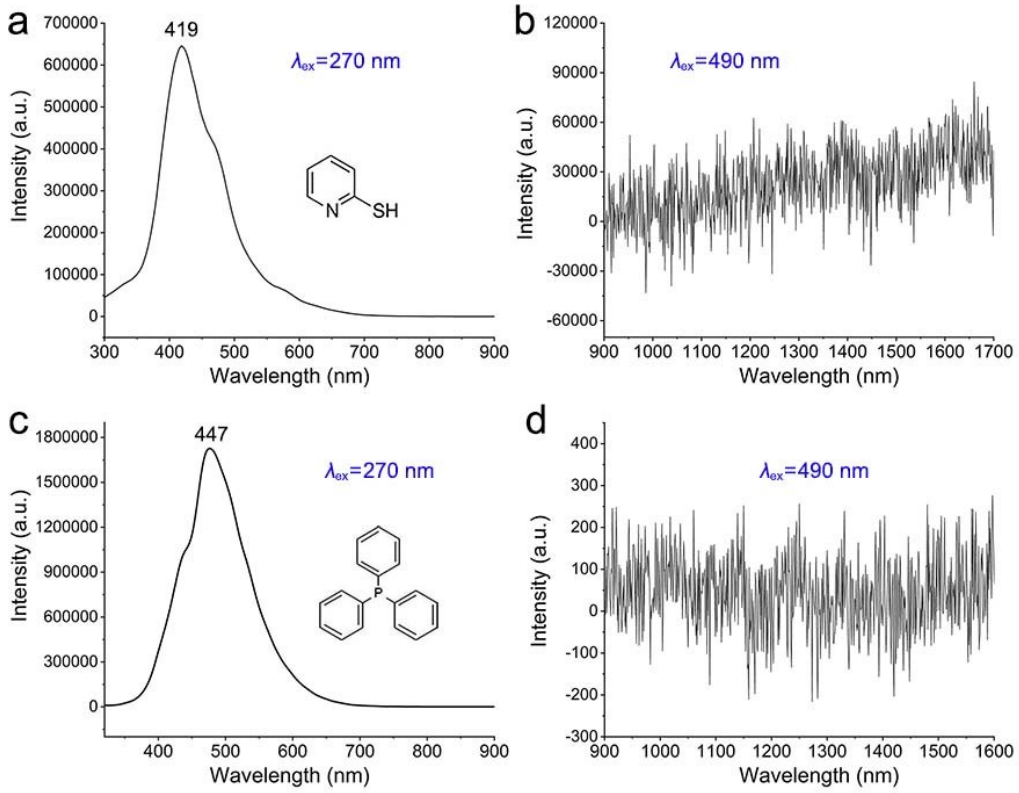

Fig. S5 Emission spectra of the ligands 2-pyridinethiol (a-b) and triphenylphosphine in DCM excited at 270 and 490 nm, respectively.

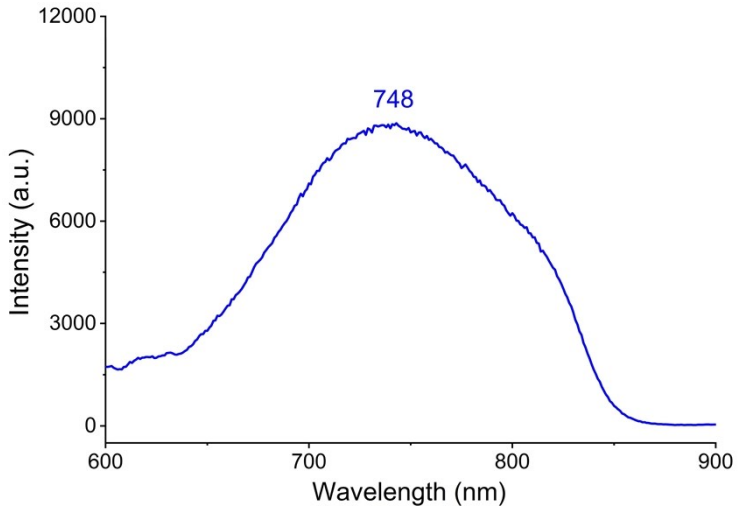

Fig. S6 Emission spectra of $[Au_{11}Cu_1(PPh_3)_7(SPy)_3]^+$ nanocluster in solid state.

S3. Calculation details

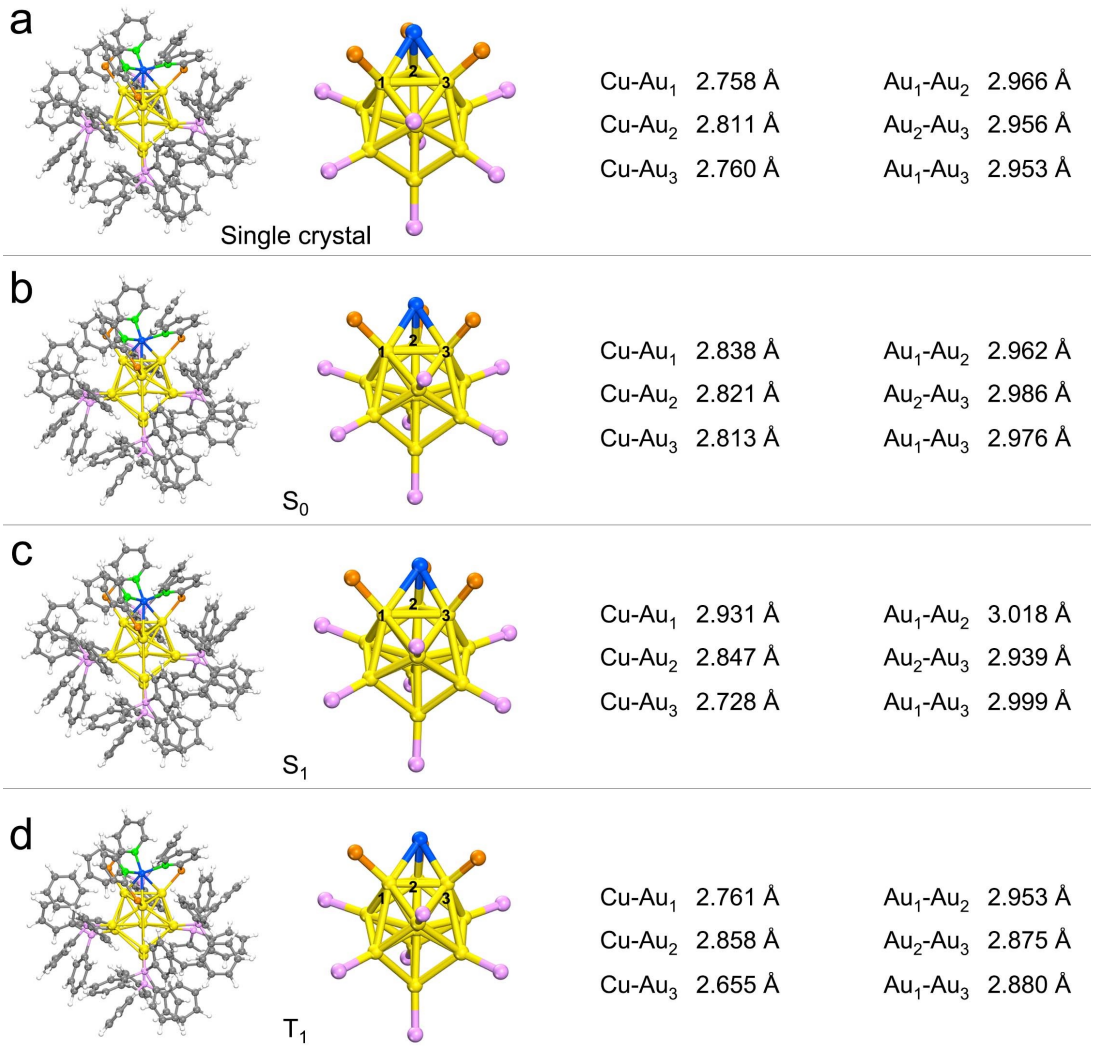

Fig. S7 The structures and bond lengths of (a) single crystal and (b-d) optimized structures at S_0, S_1, T_1 minimum. Au, yellow; Cu, blue; S, orange; P, violet; N, green; Cl, light blue; C, gray; H, white.

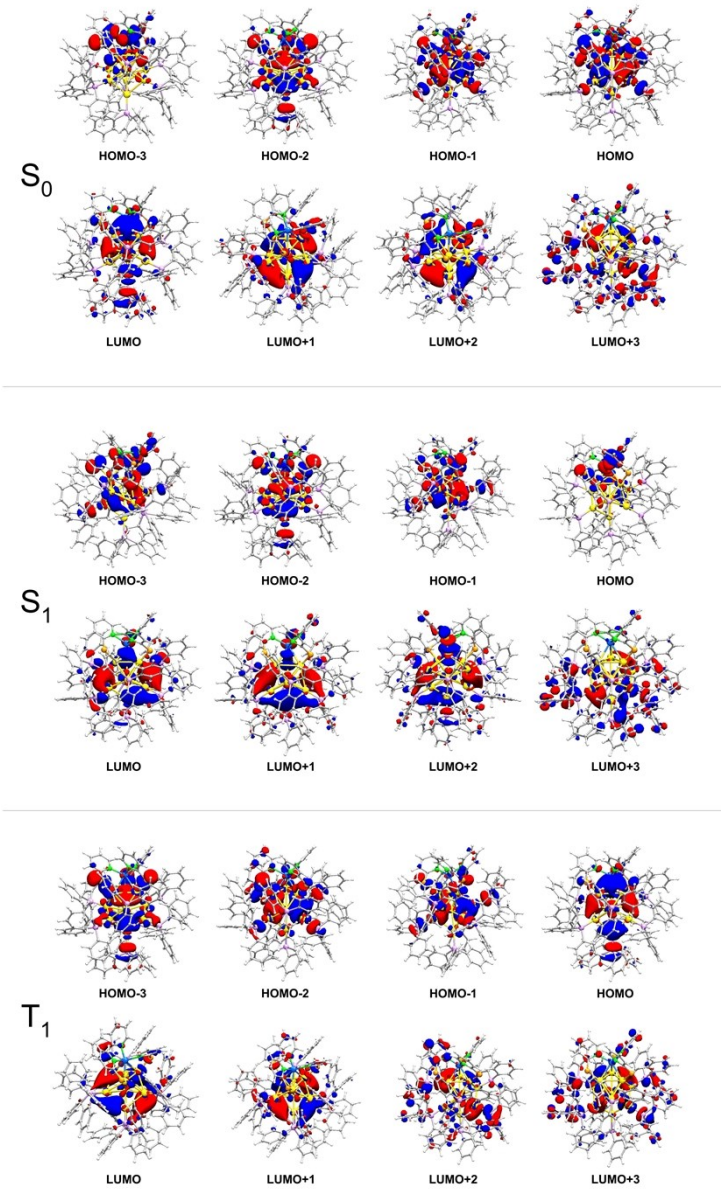

Fig. S8 Selected TD-B3LYP calculated frontier molecular orbitals at the S_0, S_1, T_1 minimum.

Table S2 TD-B3LYP computed energies at the optimized S_0, S_1 and T_1 minimum.

	Energy (hatree)	HOMO-LUMO gap (eV)
S_0	-10879.19597	2.88
S_1	-10879.13023	2.59
T_1	-10879.13479	1.08

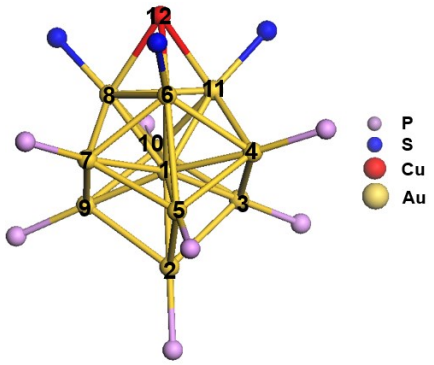

Fig. S9 The numbering of $[Au_{11}Cu_1(PPh_3)_7(SPy)_3]^+$ core at the optimized S_0 minimum.

Table S3 DFT computed $[Au_{11}Cu_1(PPh_3)_7(SPy)_3]^+$ natural population analysis (NPA) charges of several key atoms in at the optimized S_0 minimum.

Atoms	Au_1	Au_2	Au_3	Au_4	Au_5	Au_6	Au_7
NPA	-2.45	0.21	0.18	0.19	0.17	0.07	0.18
Atoms	Au_8	Au_9	Au_{10}	Au_{11}	Cu_{12}	P (avg)	S (avg)
NPA	0.06	0.18	0.19	0.07	0.52	0.92	-0.15

Table S4 TD-B3LYP computed wavelengths (nm, eV in brackets), oscillator strengths, and electronic configurations weights (in %) of strong electronic excitation transitions at the optimized S_0 minimum.

Excited state	Wavelength	Oscillator strength	Electronic configurations weights (in %)
S_1	561 (2.21)	0.0085	HOMO → LUMO (91)
S_2	559 (2.22)	0.0090	HOMO-1 → LUMO (92)
S_3	530 (2.34)	0.0025	HOMO-1 → LUMO+1 (28) HOMO → LUMO+1 (25) HOMO → LUMO+2 (25)
S_4	521 (2.38)	0.0186	HOMO-1 → LUMO+1 (30) HOMO → LUMO+2 (55)
S_5	521 (2.38)	0.0163	HOMO → LUMO+1 (62)
S_{21}	431 (2.87)	0.0557	HOMO-2 → LUMO+3 (54)

Table S5 TD-B3LYP computed wavelengths (nm, eV in brackets), oscillator strengths, and electronic configurations weights (in %) of strong electronic excitation transitions at the optimized S_1 minimum.

Excited state	Wavelength	Oscillator strength	Electronic configurations weights (in %)
S_1	634 (1.95)	0.0020	HOMO → LUMO (87)
S_2	614 (2.02)	0.0035	HOMO-1 → LUMO (95)
S_3	560 (2.21)	0.0101	HOMO → LUMO+1 (32) HOMO → LUMO+2 (35)
S_4	557 (2.22)	0.0183	HOMO-2 → LUMO (71)
S_5	548 (2.26)	0.0047	HOMO-3 → LUMO (65)

Table S6 TD-B3LYP calculated molecular orbital levels (in eV) and relevant weights (in %) with respect to Au_{11}, Cu_1, and P, S, N, C and H atoms of $[Au_{11}Cu_1(PH_3)_7(SPy)_3]^+$ at its S_0 minimum.

Orbitals	Energy (eV)	Weights (%)		
		Au_{11}	Cu_1	PSNCH
LUMO+3	-3.67	63.14	1.20	35.66
LUMO+2	-3.81	62.27	5.57	32.17
LUMO+1	-3.914	71.75	0.39	27.86
LUMO	-3.921	71.74	0.37	27.89
HOMO	-6.75	44.01	20.90	35.09
HOMO-1	-6.76	46.23	18.42	35.34
HOMO-2	-6.91	48.86	10.82	40.32
HOMO-3	-6.92	25.22	35.73	39.04
HOMO-4	-6.95	28.16	32.67	39.17
HOMO-5	-7.13	16.92	2.72	80.36
HOMO-6	-7.47	22.92	10.73	66.35
HOMO-7	-7.48	23.41	10.32	66.27
HOMO-8	-7.60	12.87	65.09	22.03
HOMO-9	-7.74	18.29	63.57	18.14
HOMO-10	-7.75	17.52	65.18	17.31
HOMO-11	-8.05	49.87	27.01	23.12
HOMO-12	-8.07	51.27	24.80	23.92
HOMO-13	-8.43	64.59	7.59	27.83

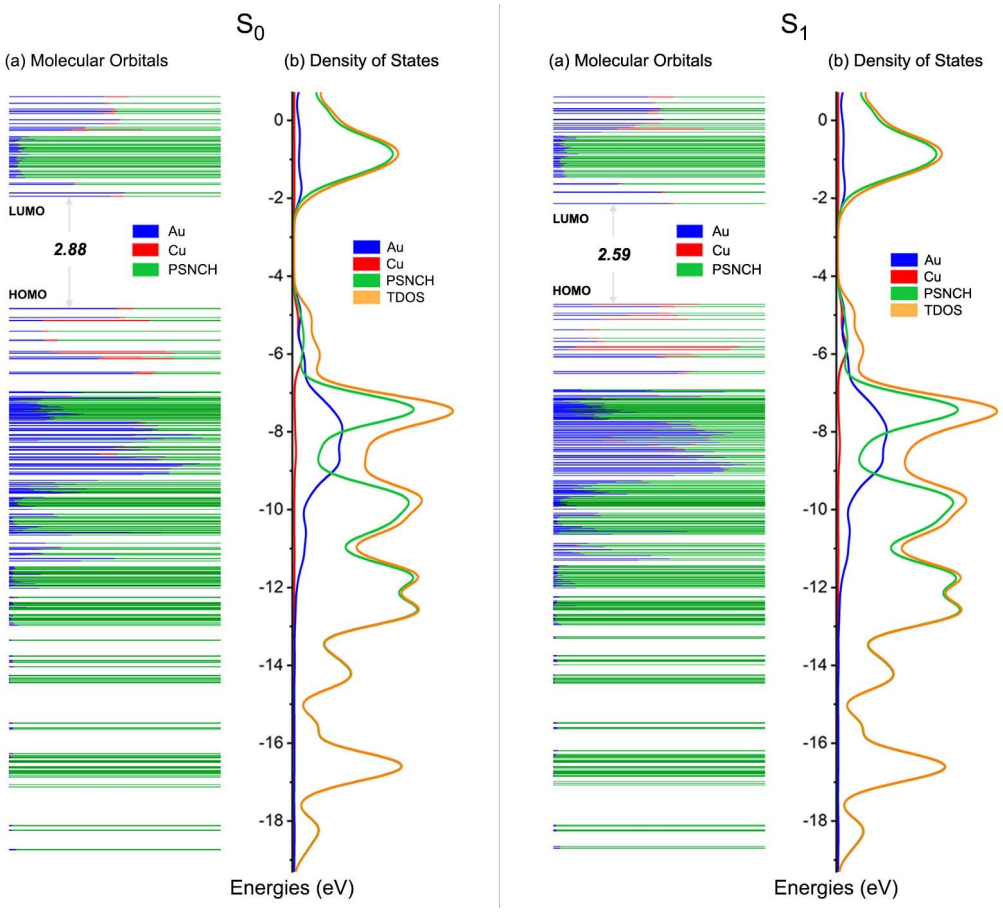

Fig. S10 (a) Kohn-Sham orbital energy level diagram and (b) total and partial density of states (DOS) of the $[Au_{11}Cu_1(PPh_3)_7(SPy)_3]^+$ at the S_0, S_1 minimum.

Table S7 TD-B3LYP calculated molecular orbital levels and relevant weights with respect to Au_{11}, Cu_1, and P, S, N, C and H atoms of $[Au_{11}Cu_1(PPh_3)_7(SPy)_3]^+$ at the S_0 and S_1 minimum.

	S_0				S_1			
Orbitals	Energy (eV)	Weights (%)			Energy (eV)	Weights (%)		
		Au_{11}	Cu_1	PSNCH		Au_{11}	Cu_1	PSNCH
LUMO+3	-1.63	30.27	0.68	69.05	-1.63	30.18	0.42	69.39
LUMO+2	-1.85	54.52	0.49	44.99	-1.84	49.59	3.30	47.11
LUMO+1	-1.86	53.46	0.51	46.03	-1.84	51.07	2.14	46.79
LUMO	-1.94	47.70	6.73	45.57	-2.13	55.08	1.96	42.96
HOMO	-4.82	50.13	8.51	41.36	-4.72	18.45	50.45	31.11
HOMO-1	-4.83	51.53	7.15	41.31	-4.78	50.84	6.89	42.28
HOMO-2	-5.06	52.02	2.83	45.16	-4.94	49.65	5.49	44.86
HOMO-3	-5.13	15.86	50.37	33.77	-5.00	34.98	23.67	41.34
HOMO-4	-5.14	16.14	50.30	33.56	-5.11	22.27	41.12	36.61
HOMO-5	-5.41	15.69	3.29	81.01	-5.37	14.42	7.55	78.04
HOMO-6	-5.63	16.27	6.77	76.97	-5.59	16.37	5.01	78.62
HOMO-7	-5.65	16.62	6.43	76.96	-5.67	20.03	4.46	75.52
HOMO-8	-5.93	19.19	54.80	26.01	-5.80	10.02	78.76	11.22
HOMO-9	-5.96	23.86	53.56	22.59	-5.82	10.72	76.32	12.96
HOMO-10	-5.97	23.14	55.32	21.54	-5.89	7.05	76.67	16.29
HOMO-11	-6.07	44.60	18.24	37.15	-6.00	52.83	12.56	34.61
HOMO-12	-6.11	42.01	35.11	22.89	-6.05	48.16	20.85	30.99
HOMO-13	-6.12	42.43	35.33	22.26	-6.08	51.65	1.63	46.73
HOMO-14	-6.45	62.31	7.60	30.09	-6.45	61.32	3.93	34.75
HOMO-15	-6.49	58.16	9.69	32.15	-6.45	64.07	4.19	31.74

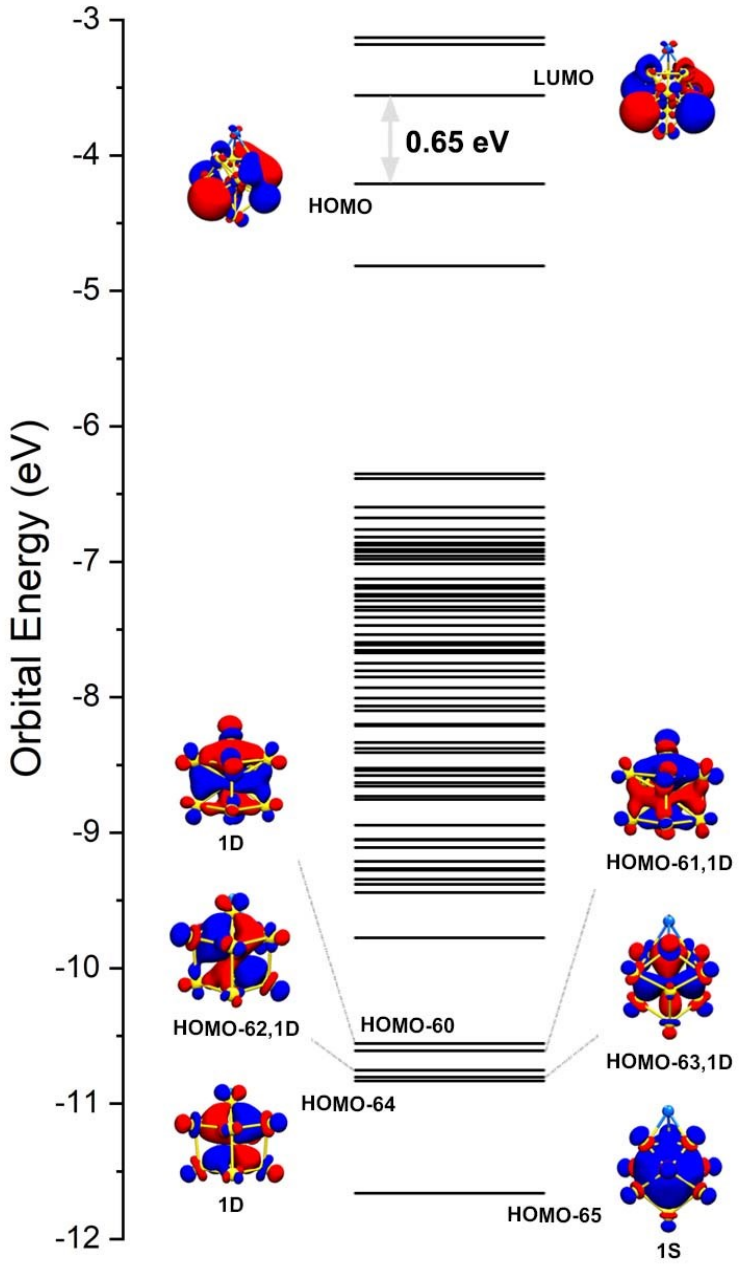

Fig. S11 The frontier molecular orbitals of the metal core $Au_{11}Cu_1$, with their superatomic features (1S, 1P, and 1D orbitals) indicated.

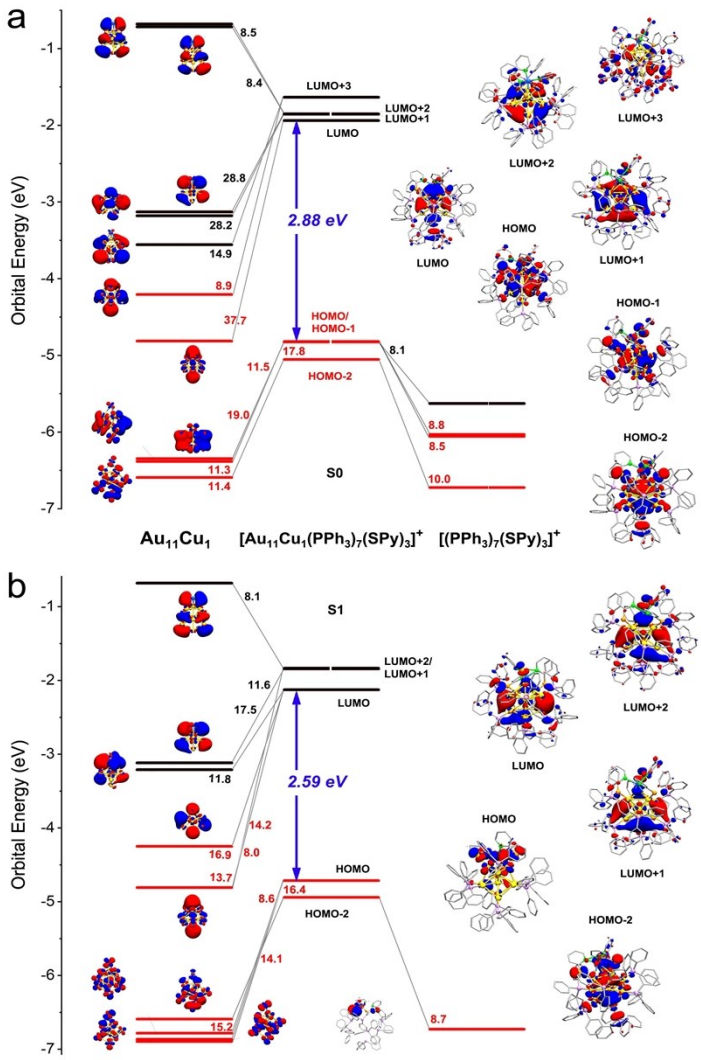

Fig. S12 Fragment analysis. Correlation of the frontier molecular orbitals of the metal core and the ligands of the $[Au_{11}Cu_1(PPh_3)_7(SPy)_3]^+$ cluster at the ground-state S_0 (a) and excitation state S_1 (b). Au yellow, Cu blue, S orange, P violet, N green, C grey. All H atoms are omitted for clarity.

Fragment orbital correlation and electronic structure analysis shows that the $Au_{11}Cu_1$ and the cationic ligands give contributions of 29.3% (17.8%+11.5%) and 16.9% (8.8%+8.1%) to the HOMO orbital at the B3LYP level, respectively, while the HOMO-1 orbital has a 30.3% (19.0%+11.3%) contribution from the neutral $Au_{11}Cu_1$ and 8.5% contribution from the cationic ligands. In comparison with their counterparts at the S_1 minimum, the nature of the LUMO at the S_1 minimum remains almost constant and it still has a much purer contribution from the metal $Au_{11}Cu_1$ core 42.4% (16.9%+11.8%+13.7%). However, the HOMO orbital has more contribution from the metal core, 40.2% (16.4%+15.2%+8.6%) in S_1 *vs.* 29.3% in S_0.